PNAS RESEARCH ARTICLE | MEDICAL SCIENCES

KRAS mutation-driven angiopoietin 2 bestows anti-VEGF resistance in epithelial carcinomas

Kayoko Hosaka[a], Patrik Andersson[a], Jieyu Wu[a], Xingkang He[a,b], Qiqiao Du[a], Xu Jing[a], Takahiro Seki[a], Juan Gao[a], Yin Zhang[c], Xiaoting Sun[a,d], Ping Huang[e], Yunlong Yang[f], Minghua Ge[g], and Yihai Cao[a,1]

Edited by Tak Mak, University of Toronto, Toronto, Canada; received March 9, 2023; accepted May 17, 2023

Defining reliable surrogate markers and overcoming drug resistance are the most challenging issues for improving therapeutic outcomes of antiangiogenic drugs (AADs) in cancer patients. At the time of this writing, no biomarkers are clinically available to predict AAD therapeutic benefits and drug resistance. Here, we uncovered a unique mechanism of AAD resistance in epithelial carcinomas with KRAS mutations that targeted angiopoietin 2 (ANG2) to circumvent antivascular endothelial growth factor (anti-VEGF) responses. Mechanistically, KRAS mutations up-regulated the FOXC2 transcription factor that directly elevated ANG2 expression at the transcriptional level. ANG2 bestowed anti-VEGF resistance as an alternative pathway to augment VEGF-independent tumor angiogenesis. Most colorectal and pancreatic cancers with KRAS mutations were intrinsically resistant to monotherapies of anti-VEGF or anti-ANG2 drugs. However, combination therapy with anti-VEGF and anti-ANG2 drugs produced synergistic and potent anticancer effects in KRAS-mutated cancers. Together, these data demonstrate that KRAS mutations in tumors serve as a predictive marker for anti-VEGF resistance and are susceptible to combination therapy with anti-VEGF and anti-ANG2 drugs.

cancer | VEGF | ANG2 | drug resistance | Ras mutation

Significance

There are urgent medical needs for the improvement of antiangiogenic cancer therapy. Defining reliable biomarkers for predicting clinical responses of antiangiogenic therapy in patients remains one of the most challenging issues for improving clinical benefits. We show our surprising finding that genetic mutation of Kirsten rat sarcoma virus (KRAS) oncogene in cancer cells switches angiogenic pathways and determines antiangiogenic drug responses. Epithelial cancers with KRAS mutations are intrinsically resistant to anti-VEGF therapy, but highly sensitive to a combination therapy with anti-VEGF and anti-ANG2 drugs. These data provide potential guidelines for the selection of subpopulations of patients to receive precision therapy of antiangiogenic drugs.

Clinically available antiangiogenic drugs (AADs), including biologics and small chemical molecules, encompass an antivascular endothelial growth factor (VEGF) component (1–3). These anti-VEGF-based AADs are widely used in the clinic for the treatment of various human cancers (1, 4–6). Despite clinical success and the development of new drugs, the overall therapeutic benefits of AADs are generally modest (1, 7). Overcoming drug resistance, including intrinsic and evasive resistance, is probably the most challenging issue for improving the survival benefits of AADs in cancer patients (8, 9). Additionally, selection of possible patient responders by defining reliable biomarkers remains a clinically unresolved issue at the time of this writing (10). Therefore, the improvement of therapeutic benefits of AADs by overcoming drug resistance and defining reliable biomarkers for patient selection remains clinically challenging and unmet urgent issues.

Cancer cells, as the result of serious genetic alterations, acquire mutations of crucially functional genes that control cell division, growth, migration, and survival (11, 12). RAS proteins belong to protooncogenes that are frequently mutated in most common human cancers, including epithelial cell–derived cancer types such as pancreatic ductal adenocarcinoma (PDAC) and colorectal cancer (CRC) (13–15). In particular, KRAS is the most commonly mutated oncogene in human epithelial cancers, followed by NRAS and HRAS (15, 16). RAS mutations have been linked to the development of drug resistance of targeted therapies that directly act on cancer cells (17–19). For example, RAS mutations in lung cancers limit clinical benefits of EGFR inhibitors by mechanisms of loss of EGFR signaling control through constitutive activation of the RAS/RAF/MEK/ERK pathway (20). Activation of RAS signaling elevates VEGF expression and drives a proangiogenic phenotype (21), suggesting that RAS-mutated tumors may have altered AAD responses. To date, the role of RAS mutations in modulating AAD sensitivity and resistance remains elusive.

Most solid tumors employ multiple angiogenic factors and cytokines to switch on angiogenesis in the tumor microenvironment (TME) (10, 22), in which VEGF and angiopoietin 2 (ANG2) are frequently up-regulated (22). While VEGF and ANG2 have overlapping functions in stimulating new vessel formation, the former is a potent driver for vessel sprouting by stimulating endothelial tips, and the latter repels perivascular cells such as pericytes from vessels to allow sprouting (23–26). Multifarious functions of VEGF, including angiogenesis, vascular permeability, hematopoiesis, immunoregulation, and neurotrophic effects, are mainly mediated by VEGFR2 tyrosine kinase receptor (6, 27–29).

Author contributions: Y.C. designed research; K.H., P.A., Q.D., T.S., Y.Z., and Y.Y. performed research; K.H., P.A., J.W., X.H., Q.D., X.J., T.S., J.G., X.S., P.H., Y.Y., M.G., and Y.C. analyzed data; K.H., P.A., J.G., Y.Z., and X.S. discussion; J.W., Q.D., X.J., T.S., P.H., Y.Y., and M.G. discussion; and K.H., X.H., and Y.C. wrote the paper.

The authors declare no competing interest.

This article is a PNAS Direct Submission.

[1]To whom correspondence may be addressed. Email: yihai.cao@ki.se.

This article contains supporting information online at https://www.pnas.org/lookup/suppl/doi:10.1073/pnas.2303740120/-/DCSupplemental.

Published July 10, 2023.

ANG2 binds to endothelial cells through relatively specific receptor Tie2 to execute its biological functions (30).

In this study, we show a unique pathway of KRAS mutation–mediated upregulation of ANG2 expression through a FOXC2 transcription–regulated mechanism. PDAC and CRC cancers with KRAS mutations are intrinsically resistant to anti-VEGF and anti-ANG2 monotherapies. However, a combination of anti-VEGF and anti-ANG2 drugs produced synergistic and potent antitumor effects. Likewise, the inactivation of KRAS resensitized $KRAS^{mut}$ tumors to anti-VEGF therapy, which was indistinguishable from $KRAS^{wt}$ tumors. On the basis of our findings, we conclude: 1) KRAS mutations may serve as a predictive marker for anti-VEGF resistance; 2) KRAS mutations augment ANG2 expression in tumors; 3) effective treatment of $KRAS^{mut}$ tumors requires a combination of anti-VEGF and anti-ANG2 drugs; and 4) inactivation of KRAS sensitizes tumors to anti-VEGF therapy.

Results

Ablation of $NG2^+$ Pericytes by Activation of RAS Oncogenes in Various Cancers. To study the impact of genetic mutations in cancer cells on tumor vasculatures, both mutant human HRAS and KRAS relative to their wild-type (wt) counterparts were used in our studies. Consistent with other previously published findings, introduction of a mutant HRAS (G12V-HRAS) into 3T3 fibroblasts induced a fibrosarcoma (31) (Fig. 1*A*). G12-HRAS-3T3 fibrosarcoma showed microvessels with high density and disorganization of tumor vasculatures (Fig. 1*A*). Surprisingly, G12-HRAS-3T3 fibrosarcomas completely lacked $NG2^+$ perivascular cells (PCs) and evaded $NG2^+$-positive signals (Fig. 1*A*).

To validate the surprising finding of PC loss in mutated RAS tumors, mutant G12-HRAS and G12V-KRAS were introduced into T241 fibrosarcoma (*SI Appendix*, Fig. S1*A*). Consistent with G12-HRAS-3T3 fibrosarcoma, G12V-HRAS-T241 and

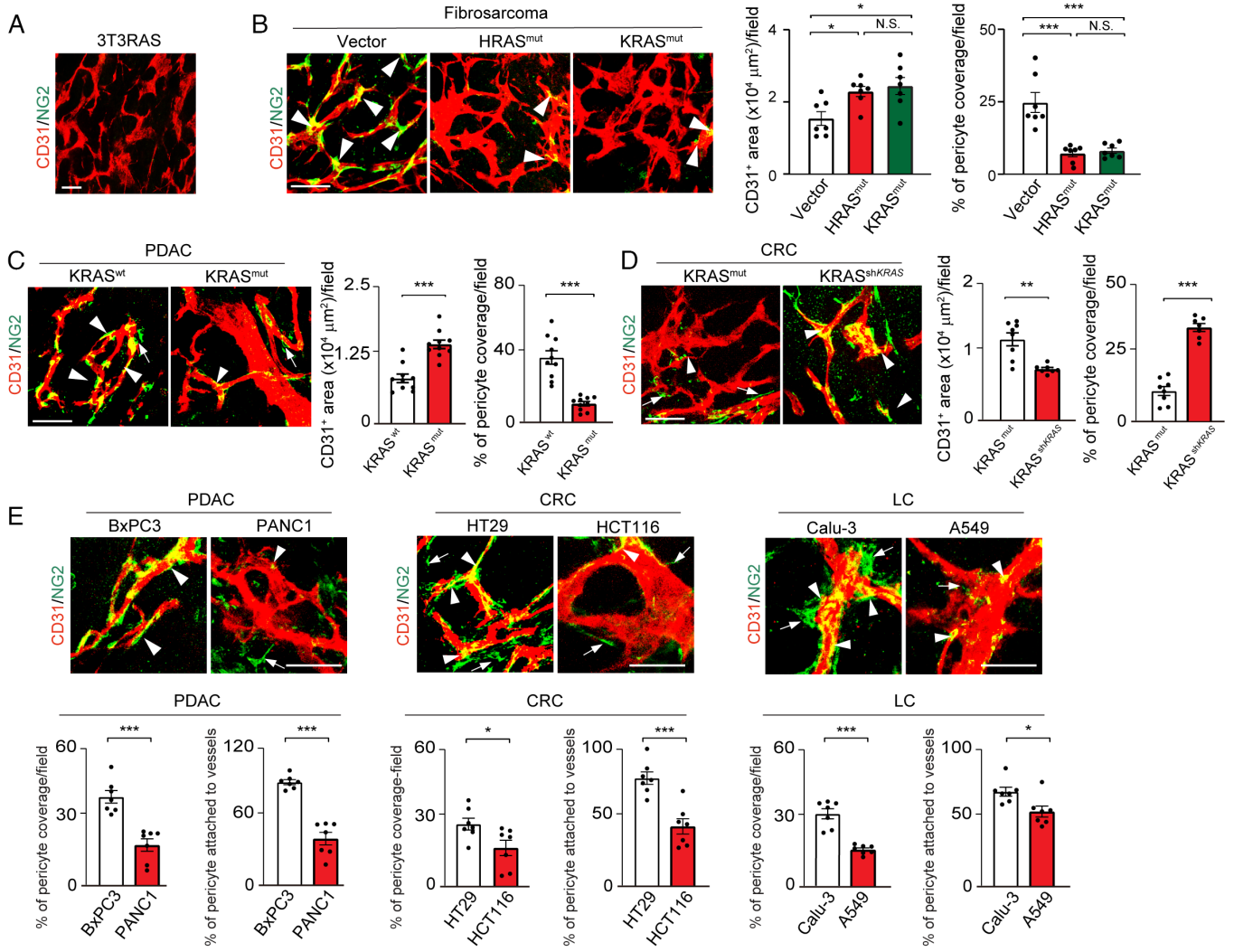

Fig. 1. Mutant RAS tumors promote pericyte ablation in tumor vasculatures. (*A*) $CD31^+$ tumor microvessels (red) and $NG2^+$ pericytes (green) in murine 3T3RAS tumor. (*B*) $CD31^+$ tumor microvessels (red) and $NG2^+$ pericytes (green) in murine T241-vector, T241-HRAS mutant, and T241-KRAS mutant tumors. Quantification of microvessel density and pericyte coverage (n = 7 random fields per group). (*C*) Tumor microvessels (red) and pericytes (green) in human BxPC3 WT and BxPC3 KRAS mutant tumors. Quantification of microvessel density and vascular coverage by pericytes (n = 10 random fields per group). (*D*) Tumor microvessels (red) and pericytes (green) in human HCT116 KRAS mutant and HCT116 sh*KRAS* tumors. Quantification of microvessel density and vascular coverage by pericytes (n = 7 to 8 random fields per group). (*E*) Tumor microvessels (red) and pericytes (green) in BxPC3 and PANC1 human PDAC tumors, HT29 and HCT116 human CRC tumors, and Calu-3 and A549 human lung tumors. Quantification of pericyte coverage and vessel-associated pericytes (n = 7 random fields per group). Arrowheads indicate vessel-associated pericytes, and arrows indicate pericytes disassociated from tumor vessels. Scale bar, 50 μm in all images. All data represent mean ± SEM. Statistical analysis was performed using one-way ANOVA followed by Tukey's multiple comparison tests (*B*) and two-sided unpaired *t* tests (*C*–*E*). $*P < 0.05$, $**P < 0.01$, $***P < 0.001$. N.S., not significant. PDAC, pancreatic ductal adenocarcinoma; CRC, colorectal carcinoma; LC, lung cancer.

G12V-KRAS-T241 fibrosarcomas also exhibited hyperneovascularization with high density of disorganized tumor vasculatures that completely lacked NG2$^+$ PCs (Fig. 1*B*).

Since KRAS mutations frequently occur in epithelial cancers such as PDACs and CRCs, we introduced G12V-KRAS into a human PDAC tumor (BxPC3) that carried wt KRAS (*SI Appendix*, Fig. S1*B*). Again, the expression of G12V-KRAS in BxPC3 tumors resulted in marked angiogenic phenotypes, disorganization of tumor vessels, and loss of NG2$^+$ PCs (Fig. 1*C*). In wt BxPC3 tumors, relative low vessel density and high proportion of NG2$^+$ PCs in association with tumor vasculatures were detected (Fig. 1*C*).

To further corroborate our findings, we employed a genetic knockdown approach using shRNA that targets KRAS in human KRAS–mutated G13D-HCT116 CRC tumors (*SI Appendix*, Fig. S1*C*). Inhibition of KRAS by a specific KRAS-shRNA restored NG2$^+$ PC coverage in tumor vessels (Fig. 1*D*). Additionally, vascular density in KRAS-shRNA HCT116 tumors was significantly reduced (Fig. 1*D*) with similar size of tumors.

To generalize our findings of RAS mutations in causing PC loss, we focused our study on KRAS mutations and compared vasculatures in paired naturally occurring tumors that carry wt and mutant KRAS. In all human tumors, including PDAC, CRC, and lung cancers, KRAS mutations augmented an angiogenic phenotype relative to the same tumors with wt KRAS (Fig. 1*E*). These human tumors with KRAS mutations contained highly dilated and disorganized vasculatures that generally lacked NG2$^+$ PCs relative to their wt controls (Fig. 1*E*).

These findings show that RAS mutations in human tumors play a causative role in ablation of perivascular cells from the tumor vasculature, and RAS mutations instigate highly disorganized tumor vasculatures.

ANG2-Dependent Perivascular Cell Ablation in KRAS Mutant Tumors. To gain mechanistic insights into KRAS mutation–instigated PC ablation, we investigated ANG2 and PDGF-B, two known growth factors committed to PC disassociation and coverage in vasculatures (30, 32, 33). In G12-HRAS- and G12V-KRAS-expressing fibrosarcomas, *Angpt2* mRNA levels were markedly elevated relative to the wt controls (Fig. 2*A*). By contrast, *Pdgfb* mRNA levels remained unchanged between mutant RAS and wt RAS tumors (Fig. 2*A*). Noticeably, treatment of G12V-KRAS-T241 fibrosarcomas with an anti-ANG2 neutralizing antibody (34, 35) restored PC coverage (Fig. 2*B*). In contrast, inhibition of PDGFRβ by a neutralizing antibody had no impact on PC coverage in G12V-KRAS-T241 fibrosarcomas (Fig. 2*B*).

Similarly, high ANG2 mRNA and protein expression levels were also detected in G12V-KRAS-BxPC3 PDAC tumors, but not in the wt-BxPC3 PDAC tumors (Fig. 2*C*). Conversely, knockdown of G13D-KRAS in HCT116 CRC tumors by a specific shRNA against KRAS markedly down-regulated ANG2 mRNA

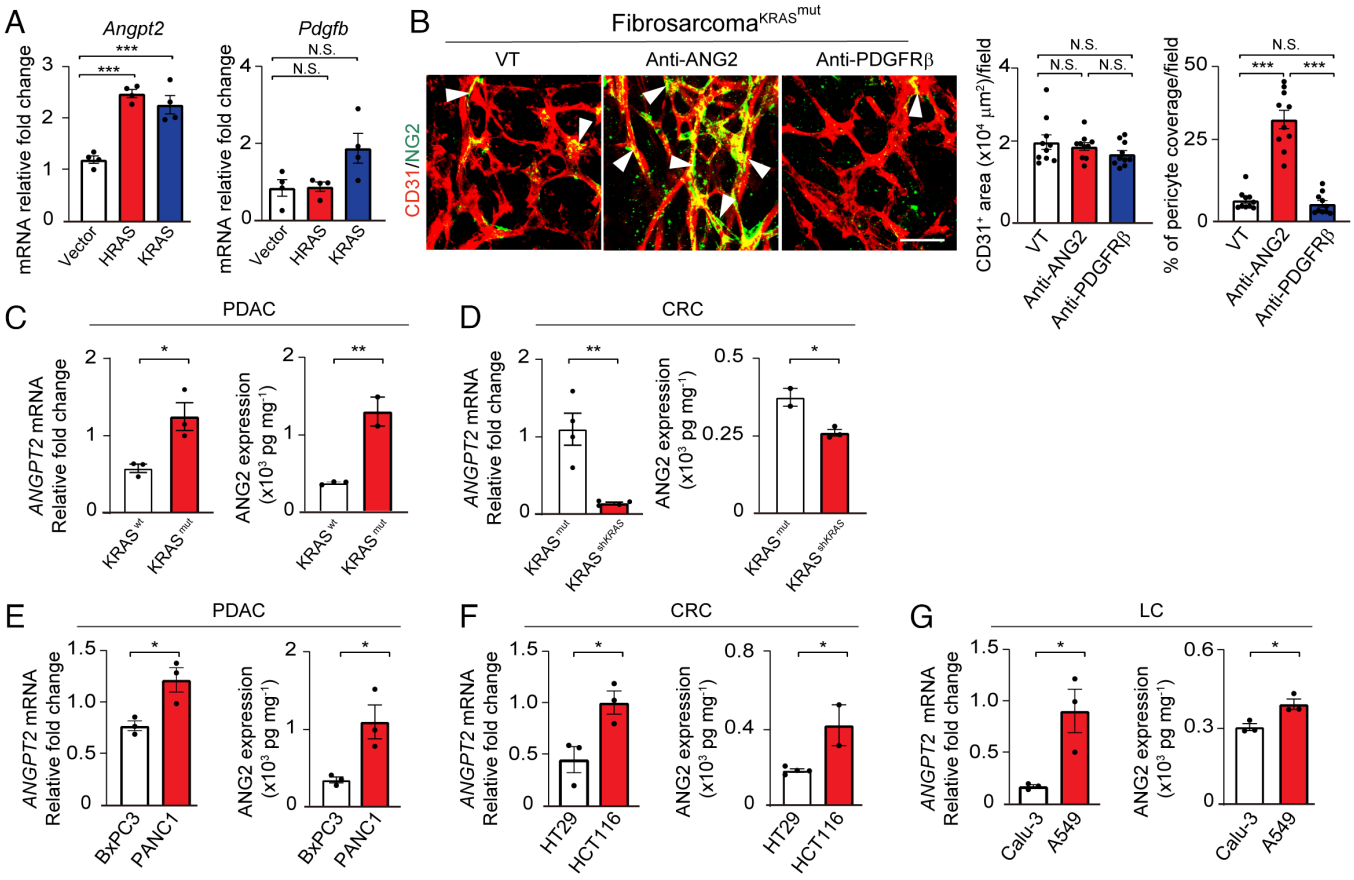

Fig. 2. Elevation of ANG2 in RAS mutant tumors. (*A*) mRNA expression of *Angpt2* and *Pdgfb* in T241-vector, T241-HRAS mutant, and T241-KRAS mutant tumors (n = 4 biological samples per group). (*B*) Tumor microvessels (red) and pericytes (green) in T241-KRAS mutant tumors treated with vehicle, an anti-ANG2 neutralizing antibody, and an anti-PDGFRβ neutralizing antibody. Quantification of microvessel density and vascular coverage by pericytes (n = 10 random fields per group). Arrowheads indicate vessel-associated pericytes. (Scale bar, 50 μm.) (*C* and *D*) *ANGPT2* mRNA expression and ANG2 protein levels in BxPC3 WT and BxPC3 KRAS mutant PDAC tumors (*C*) and HCT116 KRAS mutant and HCT116 sh*KRAS* CRC tumors (*D*) (n = 2 to 4 biological samples per group). (*E*–*G*) *ANGPT2* mRNA expression and ANG2 protein levels in BxPC3 and PANC1 PDAC tumors (*E*), HT29 and HCT116 CRC tumors (*F*), and Calu-3 and A549 lung tumors (*G*) (n = 2 to 3 biological samples per group). All data represent mean ± SEM. (Scale bar, 50 μm.) Statistical analysis was performed using one-way ANOVA followed by Tukey's multiple comparison tests (*A* and *B*) and two-sided unpaired *t* tests (*C*–*G*). **P* < 0.05, ***P* < 0.01, ****P* < 0.001. N.S., not significant. PDAC, pancreatic ductal adenocarcinoma; CRC, colorectal carcinoma; LC, lung cancer.

and protein expression levels (Fig. 2*D*). These data show that KRAS mutations augment ANG2 expression in tumor cells. In naturally occurring PDAC, CRC, and lung cancers with KRAS mutations, they all expressed high levels of ANG2 relative to their paired wt KRAS control tumors (Fig. 2 *E*–*G*). Together, these findings demonstrate a causative link between KRAS mutations and high production of ANG2.

FOXC2-Dependent Upregulation of ANG2 by KRAS Mutations. To further study the mechanism that underlay KRAS mutation–induced ANG2 expression, naturally occurring human PDAC (PANC1), CRC (HCT116), and lung cancer (A549) cells were transfected with a specific siRNA to knockdown the mutant KRAS. Expectedly, $KRAS^{mut}$ mRNAs were efficiently knocked down in these cell lines (*SI Appendix*, Fig. S2*A*). Downregulation of $KRAS^{mut}$ concordantly mitigated mRNA and protein expression levels of ANG2 in these tumor cells (Fig. 3*A*). These results further support the notion that KRAS mutations instigate ANG2 expression in various tumor cells.

Our previously published study demonstrated that the transcription factor Foxc2 targets the promoter region of the *Angpt2* gene for transcriptional upregulation of ANG2 expression (32). To investigate whether KRAS mutations potentially control FOXC2 expression, we analyzed both mRNA and protein expression levels of FOXC2 in $KRAS^{mut}$ and $KRAS^{mut\ siKRAS}$ PDAC, CRC, and lung cancers. Interestingly, knockdown of mutant KRAS substantially reduced FOXC2 mRNA and protein expression levels in these tumor cells (Fig. 3*B*). The causative link between KRAS mutations and FOXC2 expression was further validated in in vivo tumors (Fig. 3*C*).

Importantly, downregulation of FOXC2 by a specific siRNA markedly decreased ANG2 mRNA and protein expression in these $KRAS^{mut}$ tumors (Fig. 3*D* and *SI Appendix*, Fig. S2*B*). To gain further insights into signaling pathways, we studied several KRAS mutation–activated intracellular signaling components, including ERK, AKT, and NF-kB. We found that activation of ERK was a common pathway in the $KRAS^{mut}$ PDAC, CRC, and lung cancers among other signaling including AKT and NF-κB (Fig. 3*E* and *SI Appendix*, Fig. S2*C*). Having shown high ERK activation in $KRAS^{mut}$ tumors, we studied the mechanistic link between ERK activation of high ANG2 and FOXC2 expression in these tumors. Treatment of $KRAS^{mut}$ PDAC and CRC with an ERK inhibitor U0126 markedly mitigated ANG2 and FOXC2 expression (Fig. 3*F*). In summary, we have defined a signaling pathway of the KRAS–ERK–FOXC2–ANG2 axis in $KRAS^{mut}$ tumors responsible for the upregulation of ANG2.

Mechanistic Rationales of anti-VEGF and anti-ANG2 Combination Therapy. We next investigated AAD responses of tumors with wt and mutant KRAS in tumor mouse models. Stable expression of G12V-KRAS in human wt-BxPC3 resulted in marked upregulation of mRNA and protein levels of FOXC2 and ANG2 (*SI Appendix*, Figs. S1*B* and S3*A*). Consistently, G12V-KRAS-BxPC3 PDAC tumor cells exhibited high levels of phosphorylated ERKs (*SI Appendix*, Fig. S3*B*). Human wt-BxPC3 and G12V-KRAS-BxPC3 PDAC tumors were subcutaneously implanted into immunodeficient SCID mice. G12V-KRAS-BxPC3 PDAC tumors grew at an accelerated rate relative to wt-BxPC3 tumors (Fig. 4*A*). Noticeably, G12V-KRAS-BxPC3 PDAC tumors exhibited resistance to anti-VEGF and anti-ANG2 monotherapy relative to the same drug-treated wt-BxPC3 tumors (Fig. 4*B*). In the wt-BxPC3 tumors, a combination of VEGF blockade and ANG2 blockade produced no additive antitumor effects relative to anti-VEGF alone (Fig. 4*B*). In contrast, the same anti-VEGF and anti-ANG2 combination therapy produced a synergistic antitumor effect in the G12V-KRAS-BxPC3 PDAC tumors (Fig. 4*B*).

Consistent with the tumor growth rates, G12V-KRAS-BxPC3 PDAC tumors showed vascular resistance to anti-VEGF and anti-ANG2 monotherapies relative to the wt-BxPC3 tumors (Fig. 4 *C* and *D*). Intriguingly, the anti-VEGF and anti-ANG2 combination therapy markedly suppressed tumor angiogenesis in G12V-KRAS-BxPC3 PDAC tumors, which was indistinguishable from those from the combination-treated wt-BxPC3 tumors (Fig. 4 *C*–*F*). Additionally, anti-ANG2 alone completely restored PC coverage in G12V-KRAS-BxPC3 PDAC tumors (Fig. 4 *D* and *F*). Similarly, the anti-VEGF and anti-ANG2 combination therapy also restored PC coverage in G12V-KRAS-BxPC3 PDAC tumors (Fig. 4 *D* and *F*). These results demonstrate that KRAS mutations significantly contribute to drug resistance of anti-VEGF or anti-ANG2 monotherapy through tumor angiogenesis. ANG2 is responsible for PC ablation in tumors carrying KRAS mutations. A combination of anti-VEGF and anti-ANG2 produces synergistic antiangiogenic and antitumor effects in KRAS-mutated tumors.

Anti-VEGF and anti-ANG2 Combination Mitigates Tumor Vessel Permeability and Tumor Cell Proliferation. To study vascular functions of tumor microvessels, rhodamine-labeled 2,000-kDa dextran was intravenously injected into various agent-treated tumor-bearing mice. In the vehicle-treated control tumors, microvessels were partly perfused in wt-KRAS-BxPC3 PDAC (Fig. 5 *A* and *C*). Despite vascular disorganization, the perfused area of microvessels in G12V-KRAS-BxPC3 PDAC tumors was significantly increased even with the decreased perfusion ratio (Fig. 5 *B* and *C*). Treatment with VEGF blockade markedly induced the reduction of vascular perfused area regardless of improved perfusion ratio in wt-KRAS-BxPC3 PDAC (Fig. 5 *A* and *D*). However, blood perfusion in microvessels of G12V-KRAS-BxPC3 PDAC tumors remained unchanged in anti-VEGF treatment (Fig. 5 *B* and *E*). These findings show that blood perfusion in mutant KRAS tumors is intrinsically resistant to anti-VEGF therapy.

In response to anti-ANG2 treatment, the perfused microvessel area was significantly reduced despite increased perfusion ratio in wt-KRAS-BxPC3 PDAC tumors (Fig. 5 *A* and *D*). In contrast, anti-ANG2 treatment had no impact on blood perfusion in G12V-KRAS-BxPC3 PDAC tumors (Fig. 5 *B* and *E*). Notably, a combination of VEGF blockage and ANG2 blockade markedly mitigated blood perfusion area in G12V-KRAS-BxPC3 PDAC tumors (Fig. 5 *B* and *E*), whereas the same combination treatment produced a nearly indistinguishable effect on inhibition of blood perfusion area as seen in those with anti-VEGF monotherapy (Fig. 5 *A* and *D*) notwithstanding treatment-induced improvement of perfusion ratio.

In addition to alterations of vascular perfusion, AAD treatments also had functional impacts on vascular permeability. Without AAD treatment, tumor microvessels in G12V-KRAS-BxPC3 PDAC tumors were highly leaky relative to those in wt-KRAS-BxPC3 PDAC tumors (Fig. 5 *A*–*C*). Interestingly, anti-VEGF monotherapy, anti-ANG2 monotherapy, and anti-VEGF plus anti-ANG2 combination therapy markedly inhibited vascular leakiness in both wt-KRAS-BxPC3 PDAC and G12V-KRAS-BxPC3 PDAC tumors (Fig. 5 *A*, *B*, *D*, and *E*). Consistent with perfusion changes, anti-VEGF, anti-ANG2, and anti-VEGF plus anti-ANG2 treatments all increased tumor hypoxia in wt-KRAS-BxPC3 PDAC, whereas anti-VEGF plus anti-ANG2 treatment in G12V-KRAS-BxPC3 PDAC tumors produced an impact on tumor hypoxia (Fig. 5 *A*, *B*, *D*, and *E*).

Surprisingly, tumor cell proliferation in G12V-KRAS-BxPC3 PDAC tumors, as measured by $Ki67^{+}$ signals, was intrinsically

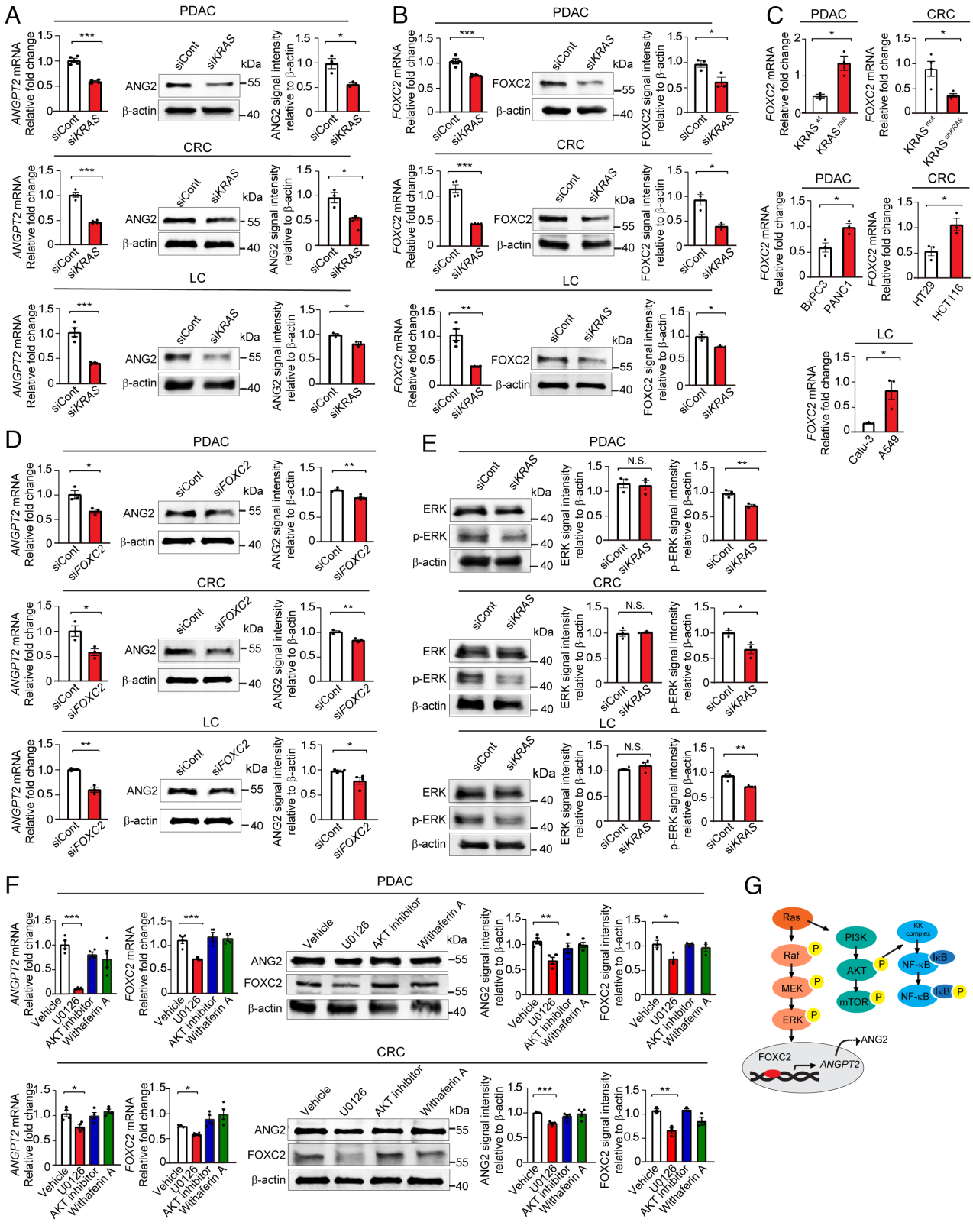

Fig. 3. KRAS mutation in tumors regulates ANG2 and FOXC2 expression through ERK signaling. (*A*) Angiopoietin 2 mRNA and protein levels in si*KRAS* transfected PANC1 PDAC, HCT116 CRC, and A549 lung tumor cell lines (n = 3 to 4 samples per group). (*B*) FOXC2 mRNA and protein levels in si*KRAS* transfected PANC1 PDAC, HCT116 CRC, and A549 lung tumor cell lines (n = 3 to 4 samples per group). (*C*) FOXC2 mRNA levels in BxPC3 WT and BxPC3 KRAS mutant PDAC tumors, HCT116 KRAS mutant and HCT116 sh*KRAS* tumors, BxPC3 and PANC1 PDAC tumors, HT29 and HCT116 CRC tumors, and Calu-3 and A549 lung tumors (n = 3 samples per group). (*D*) Angiopoietin 2 mRNA and protein levels in si*FOXC2* transfected PANC1 PDAC, HCT116 CRC, and A549 lung tumor cell lines (n = 3 samples per group). (*E*) ERK and phosphorylated-ERK protein levels in si*KRAS* transfected PANC1 PDAC, HCT116 CRC, and A549 lung tumor cell lines (n = 3 samples per group). (*F*) Angiopoietin 2 and FOXC2 mRNA and protein levels in PANC1 PDAC and HCT116 CRC tumor cell lines treated with vehicle, U0126, AKT inhibitor, and withaferin A (n = 3 to 4 per group). (*G*) Schematic diagram showing KRAS–ERK–FOXC2–ANG2 axis. All data represent mean ± SEM. Statistical analysis was performed using two-sided unpaired *t* tests (*A*–*E*) and one-way ANOVA followed by Tukey's multiple comparison tests (*F*). **P* < 0.05, ***P* < 0.01, ****P* < 0.001. N.S., not significant. P-ERK, phosphorylated-ERK. PDAC, pancreatic ductal adenocarcinoma; CRC, colorectal carcinoma; LC, lung cancer.

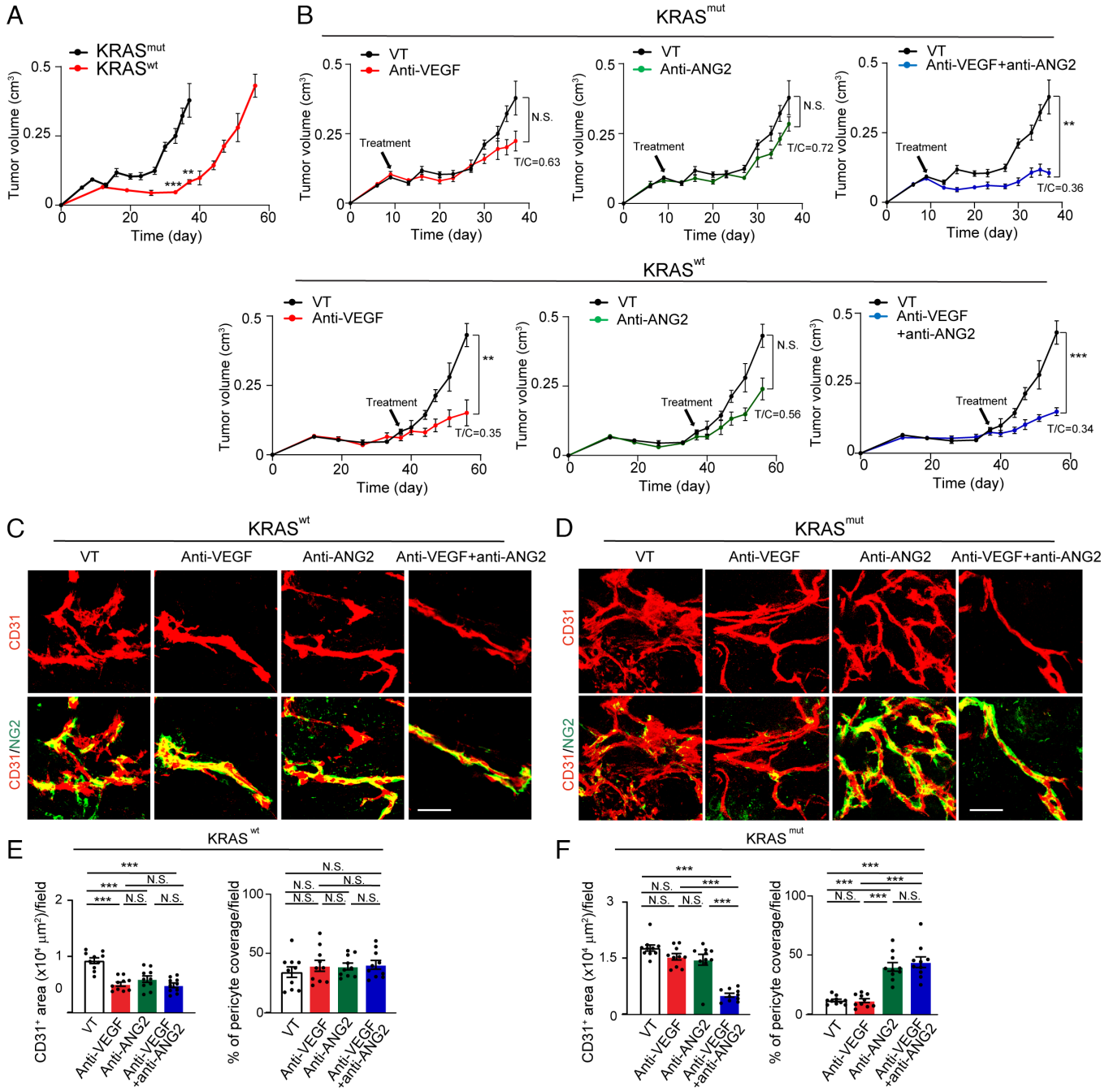

Fig. 4. Tumor growth and angiogenesis in anti-VEGF- and anti-ANG2-treated KRAS mutant PDAC tumors. (*A*) Tumor growth rates of BxPC3 KRAS wt and KRAS mutant PDAC tumors (n = 5 to 8 tumors per group). (*B*) Tumor growth rates of vehicle-, anti-VEGF-, anti-ANG2-, anti-VEGF plus anti-ANG2-treated BxPC3 KRAS wt and KRAS mutant PDAC tumors (n = 5 to 8 tumors per group). Vehicle-treated controls are the same as those in *A*. (*C* and *D*) $CD31^+$ tumor microvessels (red) and $NG2^+$ pericytes (green) in various antibody-treated BxPC3 KRAS wt (*C*) and KRAS mutant (*D*) PDAC tumors. (*E* and *F*) Quantification of microvessels and pericyte coverage in various antibody-treated BxPC3 KRAS wt (*E*) and KRAS mutant (*F*) tumors (n = 10 fields per group). All data represent mean ± SEM. (Scale bar, 50 μm.) Statistical analysis was performed using two-sided unpaired *t* tests (*A* and *B*) and one-way ANOVA followed by Tukey's multiple comparison tests (*E* and *F*). $^{**}P < 0.01$, $^{***}P < 0.001$. N.S., not significant.

resistant to anti-VEGF or anti-ANG2 monotherapy relative to those in response to the same drug-treated wt-KRAS-BxPC3 PDAC (Fig. 5 *F*–*J*). In wt-KRAS-BxPC3 PDAC tumors, anti-VEGF and anti-ANG2 combination therapy did not add additional antiproliferative effects compared with anti-VEGF monotherapy (Fig. 5 *F* and *I*). Strikingly, anti-VEGF plus anti-ANG2 combination therapy markedly inhibited tumor cell proliferation in G12V-KRAS-BxPC3 PDAC tumors, which were completely resistant to their monotherapies (Fig. 5 *G* and *J*). Similar to antiproliferative effects, the apoptotic index measured by cleaved caspase-3 markedly elevated with anti-VEGF plus anti-ANG2 combination therapy in both wt- and G12V-KRAS-BxPC3 PDAC tumors. It should be emphasized that other stromal cellular components, including tumor-associated macrophages (TAMs) and cancer-associated fibroblasts (CAFs), were not affected by AAD treatment, except G12V-KRAS-BxPC3 PDAC tumors had high contents of CAFs and TAMs (*SI Appendix*, Fig. S4). These findings demonstrate that KRAS-mutated PDAC tumors are highly sensitive to anti-VEGF plus anti-ANG2 combination therapy but are intrinsically resistant to their monotherapies.

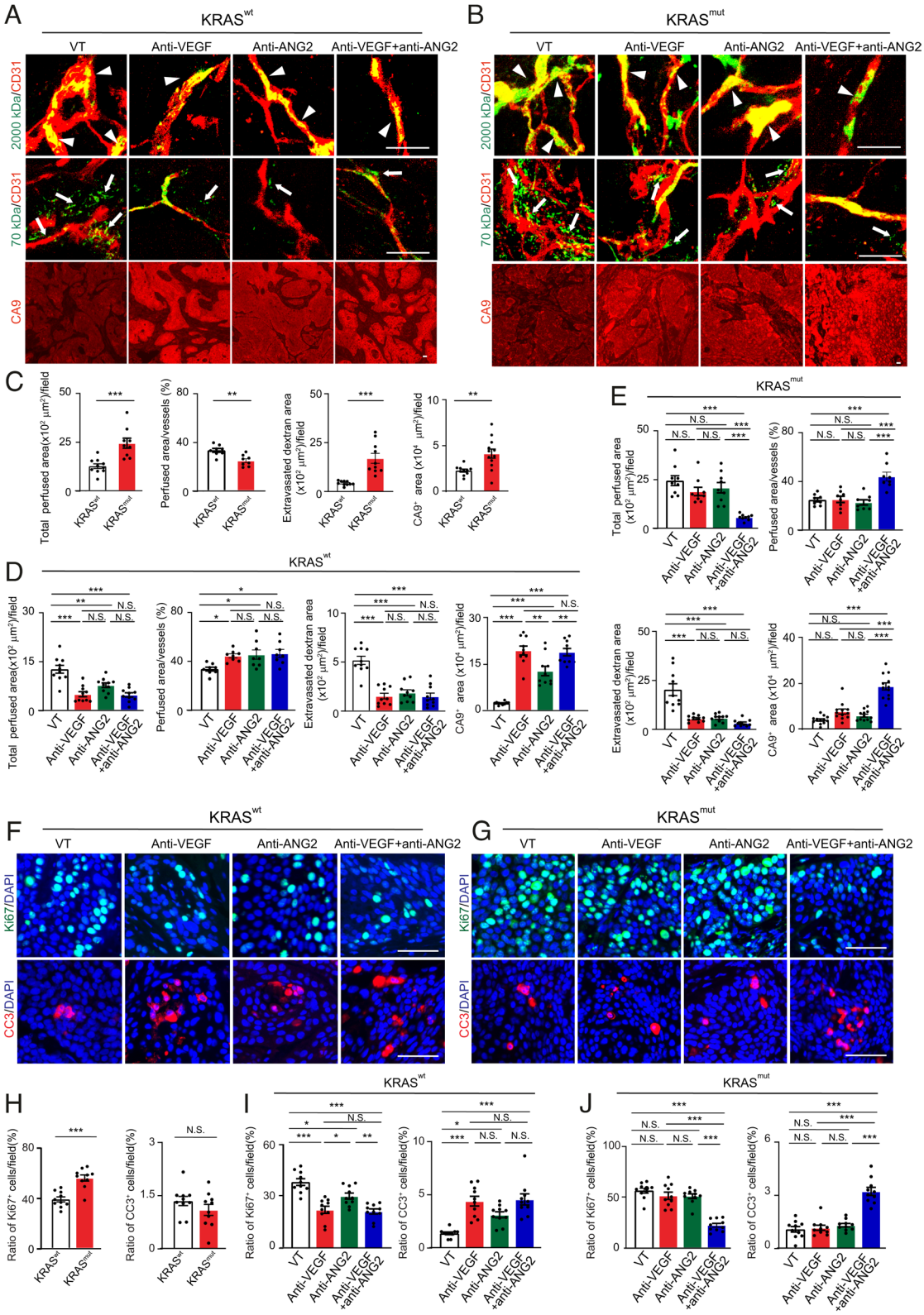

Fig. 5. Tumor vessel functions, hypoxia, and antitumor effects in various antibody-treated KRAS mutant PDAC tumors. (*A* and *B*) Vessel perfusion and permeability were analyzed by injection of rhodamine-labeled lysine 2,000 kDa and 70 kDa dextran (green) in various antibody-treated BxPC3 KRAS wt (*A*) and KRAS mutant (*B*) tumors. Microvessels (red) are counterstained. CA9 signals represent hypoxia. (*C*) Quantification of vessel perfusion area and ratio, permeability, and $CA9^+$ signals in BxPC3 KRAS wt and mutant tumors (n = 10 to 12 fields per group). (*D* and *E*) Quantification of vessel perfusion area and ratio, permeability, and $CA9^+$ signals in various antibody-treated BxPC3 KRAS wt (*D*) and KRAS mutant (*E*) tumors (n = 10 to 12 fields per group). Vehicle-treated controls are the same as those in *C*. (*F* and *G*) Proliferative (Ki67) and apoptotic (CC3) cell signals in various antibody-treated BxPC3 KRAS wt (*F*) and KRAS mutant (*G*) tumors. Nuclei are counterstained with DAPI (blue). (*H*) Quantification of $Ki67^+$ proliferative and $CC3^+$ apoptotic cell signals in BxPC3 KRAS wt and mutant tumors (n = 10 fields per group). (*I* and *J*) Quantification of $Ki67^+$ proliferative and $CC3^+$ apoptotic cell signals in various antibody-treated BxPC3 KRAS wt (*I*) and KRAS mutant (*J*) tumors (n = 10 fields per group). Vehicle-treated controls are the same as those in *H*. All data represent mean ± SEM. (Scale bar, 50 μm.) Statistical analysis was performed using two-sided unpaired *t* tests (*C* and *H*) and one-way ANOVA followed by Tukey's multiple comparison tests (*D*, *E*, *I*, and *J*). $^*P < 0.05$, $^{**}P < 0.01$, $^{***}P < 0.001$. N.S., not significant. CC3, cleaved caspase-3.

Loss of Function of Mutant KRAS Reverts Anti-VEGF Sensitivity. To further decipher KRAS mutations in contributing to anti-VEGF resistance, we took a genetic loss-of-function approach by down-regulating mutant KRAS in HCT116 CRC tumors using a specific shRNA. Downregulation of mutant KRAS in HCT116 CRC tumors resulted in decreased mRNA and protein expression levels of FOXC2 and ANG2 (*SI Appendix*, Figs. S1*C* and S5*A*). Consequently, ERK activation was also impaired in shKRAS^{mut} HCT116 CRC tumors (*SI Appendix*, Fig. S5*B*). Expectedly, knockdown of KRAS in KRAS^{mut} in HCT116 CRC tumors markedly inhibited tumor growth rates (Fig. 6*A*). KRAS^{mut}-HCT116 CRC tumors were intrinsically resistant to anti-VEGF and anti-ANG2 monotherapies (Fig. 6*B*). However, similar to the PDAC model, KRAS^{mut}-HCT116 CRC tumors were highly sensitive to the anti-VEGF plus anti-ANG2 combination therapy (Fig. 6*B*). Downregulation of mutant KRAS by shKRAS completely reverted the anti-VEGF sensitivity to the level indistinguishable from the combination therapy (Fig. 6*B*).

Consistent with the degrees of tumor suppression, downregulation of mutant KRAS sensitized the antiangiogenic effect of

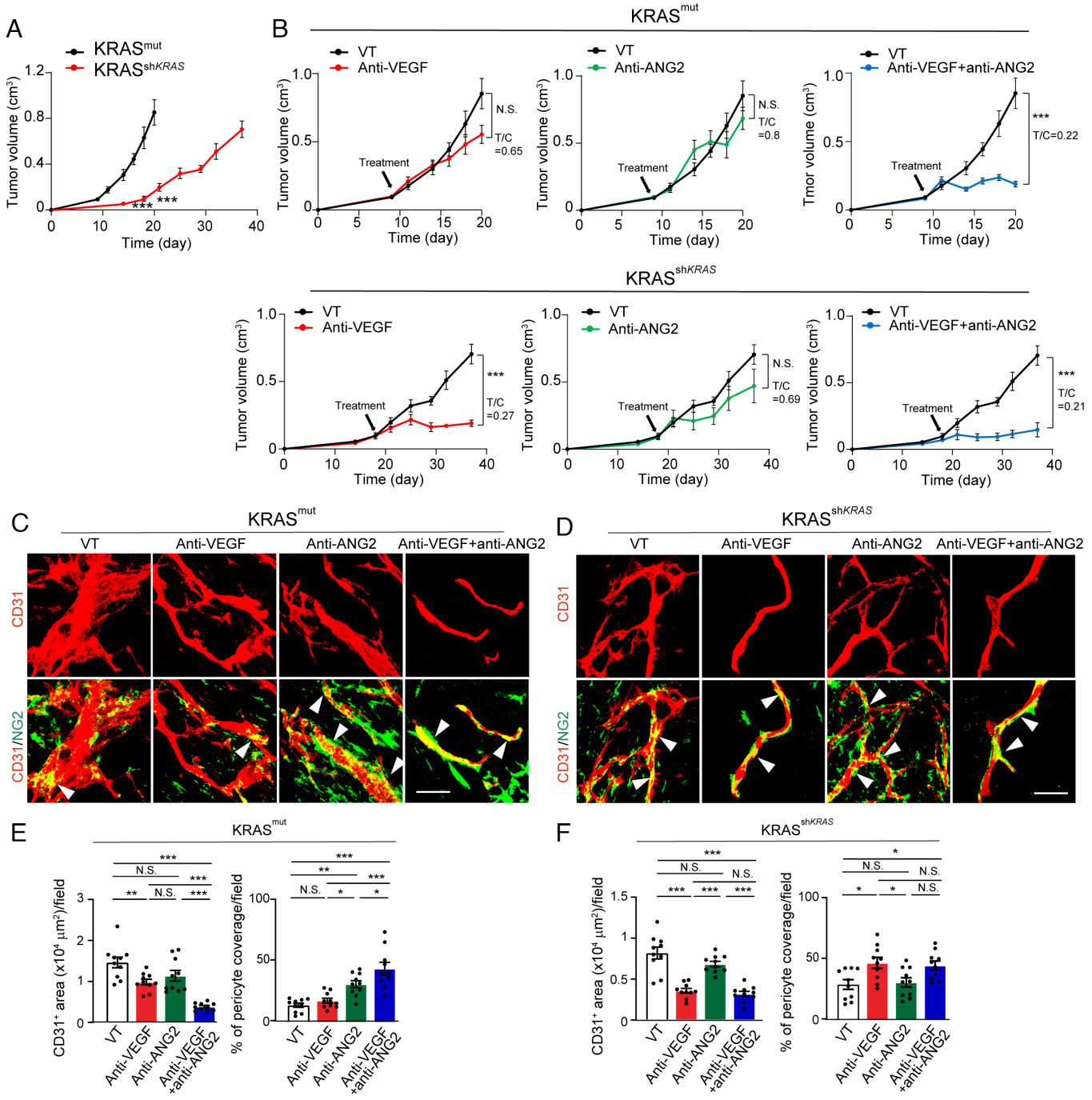

Fig. 6. Impact of *KRAS* knockdown on tumor growth, and angiogenesis in various antibody-treated CRC tumors. (*A*) Tumor growth rates of HCT116 KRAS mutant and sh*KRAS* CRC tumors (n = 5 to 8 tumors per group). (*B*) Tumor growth rates of vehicle-, anti-VEGF-, anti-ANG2-, anti-VEGF plus anti-ANG2-treated HCT116 KRAS mutant and sh*KRAS* CRC tumors (n = 5 to 8 tumors per group). Vehicle-treated controls are the same as those in *A*. (*C* and *D*) CD31$^+$ tumor microvessels (red) and NG2$^+$ pericytes (green) in various antibody-treated HCT116 KRAS mutant (*C*) and sh*KRAS* (*D*) CRC tumors. (*E* and *F*) Quantification of microvessels and pericyte coverage in various antibody-treated HCT116 KRAS mutant (*E*) and sh*KRAS* (*F*) CRC tumors (n = 10 fields per group). All data represent mean ± SEM. (Scale bar, 50 μm.) Statistical analysis was performed using two-sided unpaired *t* tests (*A* and *B*) and one-way ANOVA followed by Tukey's multiple comparison tests (*E* and *F*). $^*P < 0.05$, $^{**}P < 0.01$, $^{***}P < 0.001$. N.S., not significant.

anti-VEGF monotherapy (Fig. 6 *C*–*F*). Similar to the PDAC model, anti-ANG2 treatment markedly increased PC contents and vascular coverage in $KRAS^{mut}$-HCT116 CRC tumors (Fig. 6 *C* and *E*). In the $shKRAS^{mut}$ HCT116 CRC tumors, anti-ANG2 monotherapy had almost no impact on tumor angiogenesis, indicating that ANG2 was no longer the key driver of tumor angiogenesis (Fig. 6 *D* and *F*). Other stromal cellular components, including CAFs and TAMs, remained unchanged after treatments (*SI Appendix*, Fig. S6).

In concordance with anticancer and antiangiogenic effects, downregulation of mutant KRAS also markedly decreased total vascular perfusion area in the anti-VEGF-treated $shKRAS^{mut}$ HCT116 CRC tumors despite treatment-improved vessel perfusion ratio (Fig. 7 *A*–*E*). These anti-VEGF-treated $shKRAS^{mut}$ HCT116 CRC tumors exhibited higher degrees of tumor hypoxia (Fig. 7 *A*–*E*). Consequently, anti-VEGF monotherapy had a potent inhibitory effect on tumor cell proliferation in $shKRAS^{mut}$ HCT116 CRC tumors, which otherwise was resistant to anti-VEGF treatment without knocking down mutant KRAS (Fig. 7 *F-J*). These findings of resensitization of anti-VEGF therapy obtained from the $shKRAS^{mut}$ HCT116 CRC tumor model were reproduced by using mouse wt- and $shKRAS^{mut}$ K399 tumor models (*SI Appendix*, Fig. S7). These data indicate that KRAS mutations are mainly responsible for resistance against anti-VEGF and anti-ANG2 monotherapies.

Correlation of KRAS Mutation, ANG2 Expression, and Survival of Epithelial Cancers. To relate our findings to clinical relevance, we performed TCGA database analysis of patient cohorts of $KRAS^{wt}$ and $KRAS^{mut}$ PDACs. The total number of PDAC patients included in this study was 171 PDAC patients with 62 $KRAS^{wt}$ and 109 $KRAS^{mut}$ PDACs (Fig. 8 *A* and *B*). *ANGPT2* mRNA levels were significantly higher in the $KRAS^{mut}$ PDAC group relative to the $KRAS^{wt}$ group (Fig. 8*A*). High *ANGPT2* expression levels were positively correlated with *KRAS* expression in $KRAS^{mut}$ PDAC patients (Fig. 8*B*). Notably, high levels of *ANGPT2* were correlated with poor survivals of $KRAS^{mut}$ PDAC patients (Fig. 8*C*). Similarly, poor survival outcomes were also correlated with high *ANGPT2* expression and *KRAS* expression in KRAS mutant patients with CRC (214 patients) and lung (157 patients) cancer (Fig. 8*C*).

Discussion

Limited clinical benefits of AADs for treatments of various cancers in human patients have raised several challenging issues of antiangiogenic therapy (10). The initial idea proposed by Folkman in 1971 was that the growth of all solid tumors is dependent on angiogenesis (36). If so, inhibition of tumor angiogenesis would suppress tumor growth and be beneficial for most, if not all, tumor types. Obviously, this simplified hypothesis faces clinical challenges and cannot explain the modest clinical benefits of AADs in cancer patients. Improvement of survival benefits of AADs has become the most urgent and challenging task in antiangiogenic cancer therapy.

In clinical settings, AAD treatment of patients with already-established tumors differs from preclinical animal cancer models (37). In preclinical cancer models, antiangiogenic therapy is often initiated at the beginning of tumor formation and growth, which are completely dependent on neovascularization and lack of sufficient numbers of established tumor vasculatures (37). Probably, it is not surprising that clinically available AADs, including large biologics and small chemical tyrosine kinase inhibitors (TKIs), display potent antitumor effects in these angiogenesis-dependent preclinical cancer models. In established tumors such as those in cancer patients, tumor tissues have been vascularized at the time of diagnosis, especially in those patients with advanced cancers (37, 38). Would AADs inhibit established tumors in human patients by regression of established tumor vasculatures? To address this crucial issue, the identity of vascular survival signals that underlie maintenance of tumor vasculature should be identified.

Tumors produce multiple angiogenic factors and cytokines to instigate angiogenesis, maintain vascular survival, and remodel vasculatures. In different types of cancer, compositions of angiogenic factors and expression levels may vary considerably, depending on genetic mutations of cancer cells, stromal cellular and molecular components of the TME, and hypoxia. Even in the same type of tumors, enormous genetic and TME variations exist between patients (39). Even in the same types of cancer patients, at different stages of cancer progression, angiogenic profiles and expression levels may fluctuate substantially along with genetic mutations, composition of heterogeneous cancer cell populations, and alterations of stromal components in TME (39). Consequently, diverse beneficial responses to AADs in cancer patients may not be surprising.

The VEGF–VEGFR signaling is certainly one of the key angiogenic pathways most tumors utilize to stimulate neovascularization (40). Accumulative evidence shows that the VEGF–VEGFR2 signaling governs neovascular sprouting together with other congruently complementary signaling pathways, including the ANG1/2–TIE2, DLL4–NOTCH, and PDGF–PDGFR signaling (3). Accordingly, almost all FDA-approved AADs contain anti-VEGF components, ranging from the monospecific anti-VEGF monoclonal neutralizing antibody to broad-spectrum VEGFR-TKIs (41). Both preclinical and clinical studies show that AADs reduce vascular density and remodel existing tumor vasculatures, indicating the vascular survival and remodeling functions of VEGF (42). Although treatment of tumors with anti-VEGF AADs reduces existing tumor vasculatures, a substantial number of tumor microvessels are intrinsically resistant to anti-VEGF therapy (42). These remaining vessels are probably sufficient to maintain the tumor mass and sustain tumor growth without encountering the invasion seen in other models (43), albeit at a slower rate of growth.

In addition to the stimulation of angiogenesis, emerging evidence shows that VEGF displays multifarious functions, including vascular permeability, immunosuppression, inflammation, metabolism, endocrine regulation, neuronal regulation, and hematopoiesis (6, 27–29). Inhibition of nonangiogenic functions of VEGF by anti-VEGF AADs may potentially contribute to clinical benefits in cancer patients. Similar to VEGF, ANG2 exhibits overlapping yet distinct functions, in angiogenesis, vascular remodeling, vessel survival, and nonvascular functions (30, 44, 45). The ANG2–TIE2 signaling ablates perivascular cells from blood vessels, permitting neovascular sprouting. ANG2 also displays tumor immunosuppressive functions and may contribute to resistance to anti-VEGF and immunosuppressive drugs (46).

We previously demonstrated that FOXC2 transcriptionally targets the Ang2 promoter for upregulation of expression (32). In this study, we have uncovered the upstream signaling that up-regulates FOXC2, i.e., the activation of RAS mutation (Fig. 8*D*). Functionally active RAS mutations were accidentally discovered to cause the loss of $NG2^+$ pericytes from tumor vessels. Enforced expression of mutant RAS in cancer cells results in complete eradication of pericytes from tumor vessels. Interestingly, the total number of $NG2^+$ signals, including the vessel-disassociated positivity, is also markedly reduced (Fig. 8*D*). These findings are consistent with our previous data that perivascular cells, once detached from vessels, may differentiate into other cell types such as fibroblasts, a process designated as pericyte–fibroblast transition (47). On the basis of these findings,

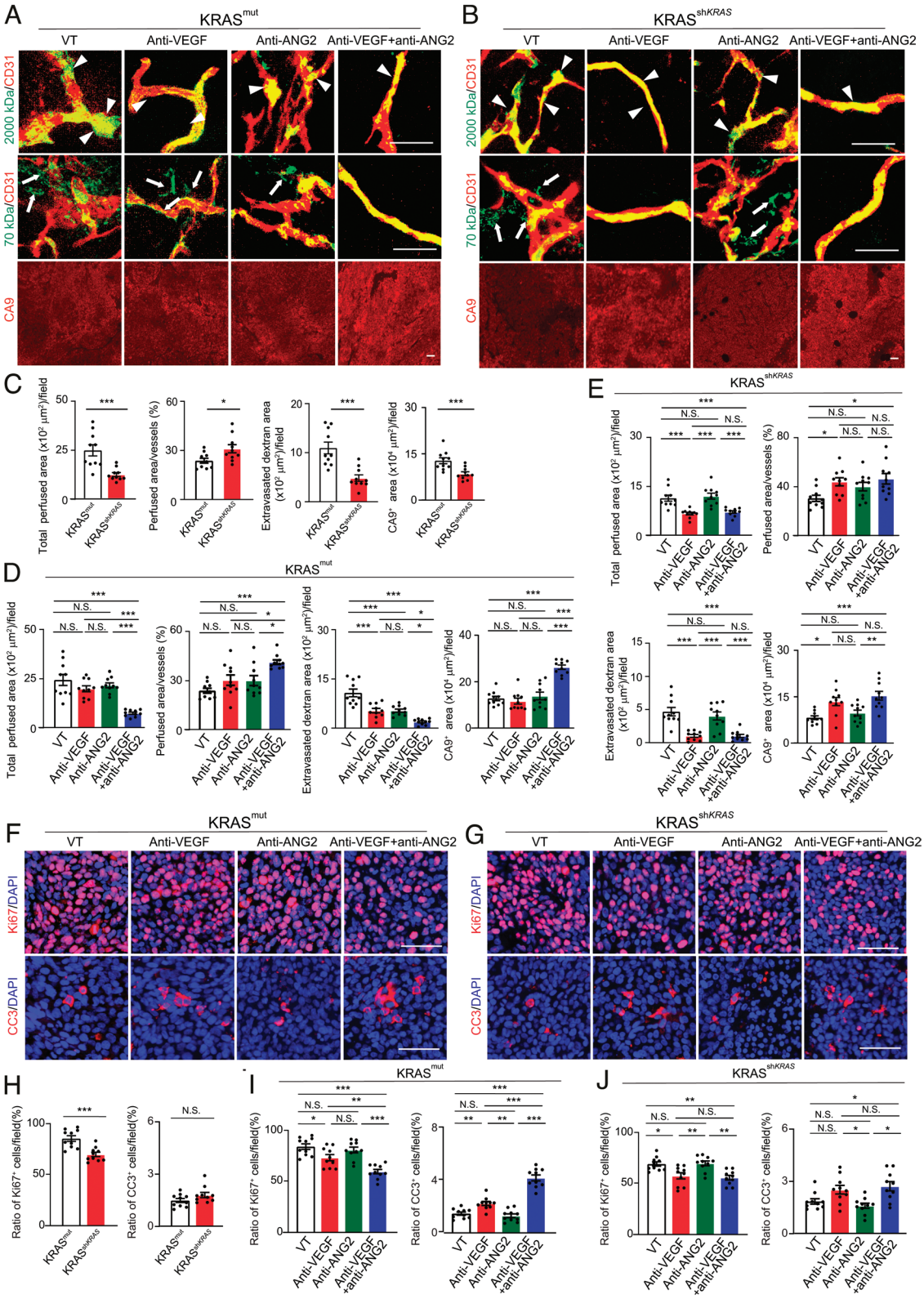

Fig. 7. Tumor vessel functions, hypoxia, and antitumor effects on sh*KRAS* CRC tumors in response to various antibody treatments. (*A* and *B*) Vessel perfusion and permeability were analyzed by injection of rhodamine-labeled lysine 2,000 kDa and 70 kDa dextran (green) in HCT116 KRAS mutant (*A*) and sh*KRAS* (*B*) CRC tumors. Microvessels (red) are counterstained. CA9 signals represent hypoxia. (*C*) Quantification of vessel perfusion area and ratio, permeability, and $CA9^+$ signals in HCT116 KRAS mutant and sh*KRAS* CRC tumors (n = 10 fields per group). (*D* and *E*) Quantification of vessel perfusion area and ratio, permeability, and $CA9^+$ signals in various antibody-treated HCT116 KRAS mutant (*D*) and sh*KRAS* (*E*) tumors (n = 10 to 12 fields per group). Vehicle-treated controls are the same as those in *C*. (*F* and *G*) Proliferative (Ki67) and apoptotic (CC3) cell signals in various antibody-treated HCT116 KRAS mutant (*F*) and sh*KRAS* (*G*) CRC tumors. Nuclei are counterstained with DAPI (blue). (*H*) Quantification of $Ki67^+$ proliferative and $CC3^+$ apoptotic cell signals in HCT116 KRAS mutant and sh*KRAS* CRC tumors (n = 10 fields per group). (*I* and *J*) Quantification of $Ki67^+$ proliferative and $CC3^+$ apoptotic cell signals in various antibody-treated HCT116 KRAS mutant (*I*) and sh*KRAS* (*J*) CRC tumors (n = 10 fields per group). Vehicle-treated controls are the same as those in *H*. All data represent mean ± SEM. (Scale bar, 50 μm.) Statistical analysis was performed using two-sided unpaired *t* tests (*C* and *H*) and one-way ANOVA followed by Tukey's multiple comparison tests (*D*, *E*, *I*, and *J*). $*P < 0.05$, $**P < 0.01$, $***P < 0.001$. N.S., not significant. CC3, cleaved caspase-3.

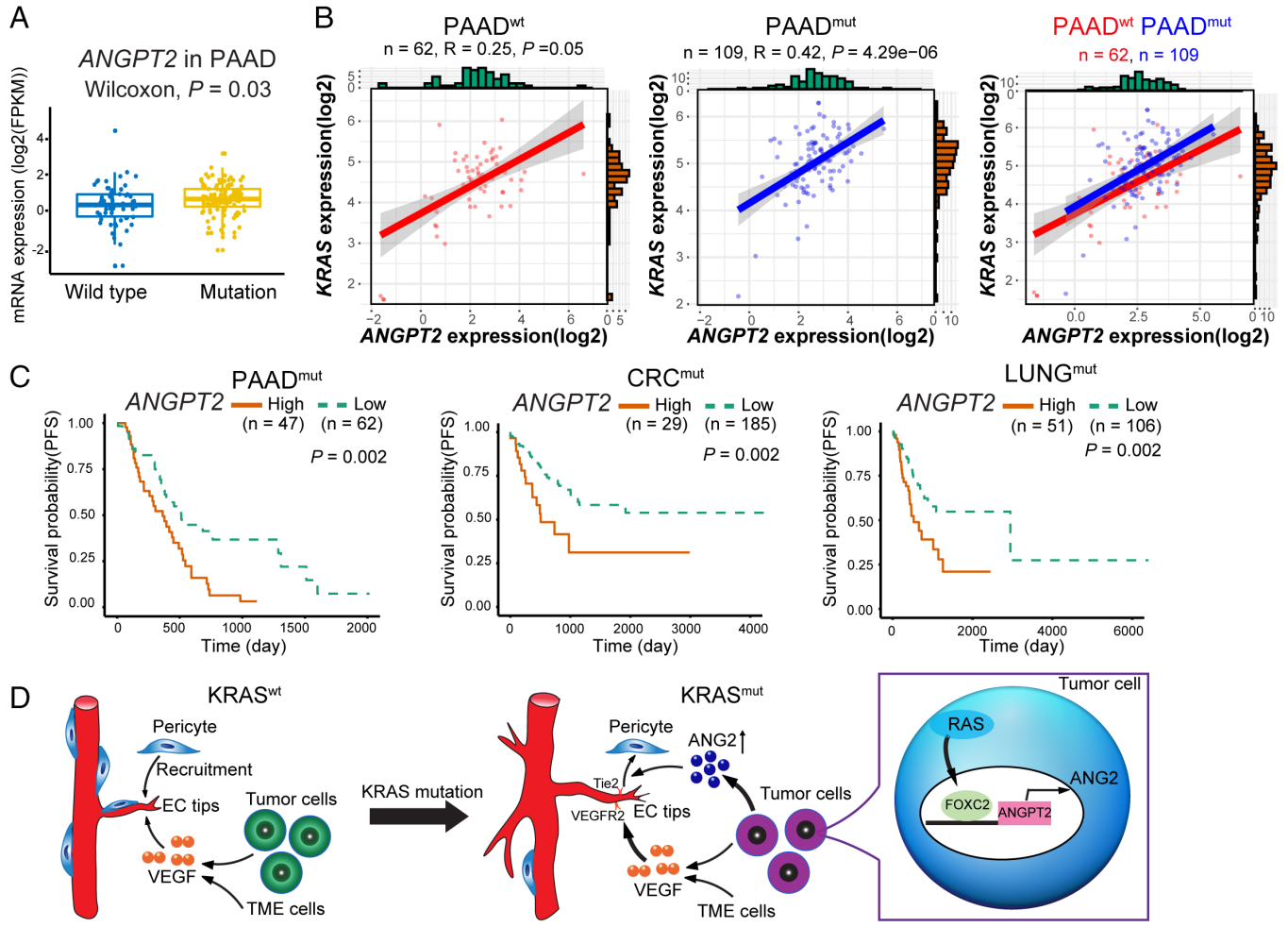

Fig. 8. Correlation, survivals, and schematic diagram of KRAS mutant tumor–induced anti-VEGF resistance mechanisms. (*A*) *ANGPT2* expression levels in KRAS wt and mutant PDAC patients (PAAD, n = 61 vs. 109, *P* = 0.003). (*B*) Correlation of *ANGPT2* and *KRAS* expression in KRAS wt (n = 62, *P* = 0.05) and mutant (n = 109, *P* = 4.29e-06) PDAC patients. (*C*) Kaplan–Meier survival of *ANGPT2*-high vs. *ANGPT2*-low PAAD (n = 47 vs. 62, *P* = 0.002); CRC (n = 29 vs. 185, *P* = 0.002); and LUAD (n = 51 vs. 106, *P* = 0.002) of KRAS mutant cases. (*D*) Schematic diagram of KRAS mutant tumors in promoting pericyte-loss tumor vasculatures. In KRAS wt tumors, tumor- and the TME-derived VEGF promotes tumor angiogenesis, and pericytes are recruited to coat tumor vessels. In contrast, KRAS mutant tumors generate a pericyte-impaired phenotype by increasing tumor-derived ANG2 through the RAS–FOXC2–ANG2 axis, leading to accelerated angiogenesis by sustainable VEGF access to endothelial cells. PAAD, pancreatic cancer; CRC, colorectal cancer; LUNG, lung cancer

mutant RAS proteins may augment tumor angiogenesis through two mechanisms: 1) enhancing VEGF-induced angiogenesis by upregulation of VEGF expression; and 2) activating the FOXC2–ANG2 signaling. Both VEGF and ANG2 induce vascular permeability through, albeit different mechanisms, separating endothelial junctions and fenestrae by the former and ablating perivascular cells by the latter (Fig. 8*D*). Another interesting possibility is that in response to antiangiogenic therapy, reactive oxygen species also play a role in the regulation of ANG2 (48).

Although angiogenic endothelial cells have been described as the major cellular source of ANG2 in tumors, various tumor cells do produce ANG2 (48–53). To the best of our knowledge, genetic mutations in tumor cells have not been specifically linked to ANG2 production. Despite the development of various ANG2 inhibitors for clinical use (35), these inhibitors produce limited clinical benefits (54, 55). In addition, dual targeting of VEGF and ANG2 by a bispecific antibody has not been shown to produce additional benefits above anti-VEGF monotherapy in patients with metastatic CRC (56). As discussed above, cancers are heterogeneous diseases and even in the same type of cancer, tremendous heterogeneity exists. In these clinical trials, survival benefits of ANG2 inhibitors in relation to RAS mutations have not been evaluated. Roughly 50% of CRC patients carry KRAS mutations (16), and their responses to ANG2 inhibitors, either monotherapy or combination with anti-VEGF drugs, warrant separate clinical studies. Furthermore, the increased ANG2 levels in KRAS-mutant PDAC patients (Fig. 8*A*) may be related to intertumoral angiogenic hot spots or involvement of other TME components as PDAC expressed low levels of angiogenesis. Moreover, although our current findings are focused on KRAS mutations, simultaneous targeting of VEGF and ANG2 for effective antiangiogenic therapy may also apply to other cancer types with HRAS or NRAS mutations.

Together, our findings provide mechanistic insights into genetic mutations and AAD resistance. On the basis of these data, we propose that dual targeting VEGF and ANG2 should be particularly beneficial for a subset of patients with functional RAS mutations.

Materials and Methods

Animals, Xenograft Tumor Models, and Treatment. All animal studies were approved by the North Stockholm Animal Ethical Committee, Stockholm, Sweden. C57BL/6 and severe combined immunodeficiency (SCID) strains were bred in the animal facility of the Department of Microbiology, Tumor and Cell Biology, Karolinska Institute, Stockholm, Sweden. Four- to 6-wk-old C57BL/6 and 6- to 8-wk-old SCID mice were used for experiments.

Statistics. Statistical analysis of experimental results was performed using a two-sided unpaired *t* test and one-way ANOVA followed by Tukey's multiple comparison tests. $*P < 0.05$, $**P < 0.01$, and $***P < 0.001$ were considered significant. N.S.= not significant.

More details are provided in *SI Appendix, Materials and Methods*.

Data, Materials, and Software Availability. All study data are included in the article and/or *SI Appendix*.

ACKNOWLEDGMENTS. Yihai Cao's laboratory is supported through research grants from the European Research Council advanced grant ANGIOFAT (Project no. 250021), the Swedish Research Council, the Swedish Cancer Foundation, the Swedish Children's Cancer Foundation, the Strategic Research Areas–Stem Cell and Regenerative Medicine Foundation, the Karolinska Institute Foundation, the Karolinska Institute distinguished professor award, the Torsten Soderbergs Foundation, the Maud and Birger Gustavsson Foundation, the NOVO Nordisk Foundation-Advance grant, the NOVO Nordisk Foundation, and the Knut and Alice Wallenberg's Foundation. This study was supported by grants from the National Key R&D Program of China (2020YFC0846600).

Author affiliations: [a]Department of Microbiology, Tumor and Cell Biology, Karolinska Institute, Stockholm 171 65, Sweden; [b]Department of Gastroenterology, Sir Run Run Shaw Hospital, Zhejiang University School of Medicine, Hangzhou, Zhejiang 310016, China; [c]School of Pharmacology, Binzhou Medical University, Yantai, Shandong 264003, China; [d]Oujiang Laboratory (Zhejiang Lab for Regenerative Medicine, Vison and Brain Health), School of Pharmaceutical Science, Wenzhou Medical University, Wenzhou 325024, China; [e]Department of Pharmacy, Zhejiang Provincial People's Hospital, People's Hospital of Hangzhou Medical College, Hangzhou 310053, China; [f]Department of Cellular and Genetic Medicine, School of Basic Medical Sciences, Fudan University, Shanghai 200032, China; and [g]Department of Head, Neck and Thyroid Surgery, Zhejiang Provincial People's Hospital, People's Hospital of Hangzhou Medical College, Hangzhou 31003, China

1. R. S. Kerbel, Antiangiogenic therapy: A universal chemosensitization strategy for cancer? *Science* **312**, 1171–1175 (2006).
2. B. Al-Husein *et al.*, Antiangiogenic therapy for cancer: An update. *J. Hum. Pharmacol.* **32**, 1095–1111 (2012).
3. G. Niu, X. Chen, Vascular endothelial growth factor as an anti-angiogenic target for cancer therapy. *Curr. Drug Targets* **11**, 1000–1017 (2010).
4. L. Rosen, Antiangiogenic strategies and agents in clinical trials. *Oncologist* **5**, 20–27 (2000).
5. J. Welti, S. Loges, S. Dimmeler, P. Carmeliet, Recent molecular discoveries in angiogenesis and antiangiogenic therapies in cancer. *J. Clin. Invest.* **123**, 3190–3200 (2013).
6. Y. Yang, Y. Cao, The impact of VEGF on cancer metastasis and systemic disease. *Semin. Cancer Biol.* **86**, 251–261 (2022), 10.1016/j.semcancer.2022.03.011.
7. Y. Cao, Antiangiogenic cancer therapy. *Semin. Cancer Biol.* **14**, 139–145 (2004), 10.1016/j.semcancer.2003.09.018.
8. J. M. Ebos, C. R. Lee, R. S. Kerbel, Tumor and host-mediated pathways of resistance and disease progression in response to antiangiogenic therapy. *Clin. Cancer Res.* **15**, 5020–5025 (2009).
9. G. Bergers, D. Hanahan, Modes of resistance to anti-angiogenic therapy. *Nat. Rev. Cancer* **8**, 592–603 (2008).
10. Y. Cao, W. Zhong, Y. Sun, Improvement of antiangiogenic cancer therapy by understanding the mechanisms of angiogenic factor interplay and drug resistance. *Semin. Cancer Biol.* **19**, 338–343 (2009), 10.1016/j.semcancer.2009.05.001.
11. P. A. Futreal *et al.*, A census of human cancer genes. *Nat. Rev. Cancer* **4**, 177–183 (2004).
12. C. Greenman *et al.*, Patterns of somatic mutation in human cancer genomes. *Nature* **446**, 153–158 (2007).
13. I. A. Prior, P. D. Lewis, C. Mattos, A comprehensive survey of Ras mutations in cancer. *Cancer Res.* **72**, 2457–2467 (2012).
14. J. L. Bos, Ras oncogenes in human cancer: A review. *Cancer Res.* **49**, 4682–4689 (1989).
15. A. D. Cox, S. W. Fesik, A. C. Kimmelman, J. Luo, C. J. Der, Drugging the undruggable RAS: Mission possible? *Nat. Rev. Drug Discov.* **13**, 828–851 (2014), 10.1038/nrd4389.
16. S. R. Punekar, V. Velcheti, B. G. Neel, K. K. Wong, The current state of the art and future trends in RAS-targeted cancer therapies. *Nat. Revs. Clin. Oncol.* **19**, 637–655 (2022), 10.1038/s41571-022-00671-9.
17. W. De Roock, V. De Vriendt, N. Normanno, F. Ciardiello, S. Tejpar, KRAS, BRAF, PIK3CA, and PTEN mutations: Implications for targeted therapies in metastatic colorectal cancer. *Lancet Oncol.* **12**, 594–603 (2011).
18. H. Linardou *et al.*, Assessment of somatic k-RAS mutations as a mechanism associated with resistance to EGFR-targeted agents: A systematic review and meta-analysis of studies in advanced non-small-cell lung cancer and metastatic colorectal cancer. *Lancet Oncol.* **9**, 962–972 (2008).
19. Y. Qian *et al.*, Molecular alterations and targeted therapy in pancreatic ductal adenocarcinoma. *J. Hematol. Oncol.* **13**, 1–20 (2020).
20. M. Raponi, H. Winkler, N. C. Dracopoli, KRAS mutations predict response to EGFR inhibitors. *Curr. Opin. Pharmacol.* **8**, 413–418 (2008).
21. J. Rak *et al.*, Mutant ras oncogenes upregulate VEGF/VPF expression: Implications for induction and inhibition of tumor angiogenesis. *Cancer Res.* **55**, 4575–4580 (1995).
22. M. De Palma, D. Biziato, T. V. Petrova, Microenvironmental regulation of tumour angiogenesis. *Nat. Rev. Cancer* **17**, 457–474 (2017).
23. H. Gerhardt *et al.*, VEGF guides angiogenic sprouting utilizing endothelial tip cell filopodia. *J. Cell Biol.* **161**, 1163–1177 (2003).
24. P. Vajkoczy *et al.*, Microtumor growth initiates angiogenic sprouting with simultaneous expression of VEGF, VEGF receptor-2, and angiopoietin-2. *J. Clin. Invest.* **109**, 777–785 (2002).
25. U. Fiedler *et al.*, The Tie-2 ligand angiopoietin-2 is stored in and rapidly released upon stimulation from endothelial cell Weibel-Palade bodies. *Blood* **103**, 4150–4156 (2004).
26. A. Armulik, A. Abramsson, C. Betsholtz, Endothelial/pericyte interactions. *Cric. Res.* **97**, 512–523 (2005).
27. J. E. Ohm *et al.*, VEGF inhibits T-cell development and may contribute to tumor-induced immune suppression. *Blood* **101**, 4878–4886 (2003).
28. J. Gavard, J. S. Gutkind, VEGF controls endothelial-cell permeability by promoting the β-arrestin-dependent endocytosis of VE-cadherin. *Nat. Cell Biol.* **8**, 1223–1234 (2006).
29. O. O. Ogunshola *et al.*, Paracrine and autocrine functions of neuronal vascular endothelial growth factor (VEGF) in the central nervous system. *J. Biol. Chem.* **277**, 11410–11415 (2002).
30. A. Armulik, A. Abramsson, C. Betsholtz, Endothelial/pericyte interactions. *Circ. Res.* **97**, 512–523 (2005), 10.1161/01.RES.0000182903.16652.d7.
31. J. Rak *et al.*, Oncogenes and tumor angiogenesis: Differential modes of vascular endothelial growth factor up-regulation in ras-transformed epithelial cells and fibroblasts. *Cancer Res.* **60**, 490–498 (2000).
32. Y. Xue *et al.*, FOXC2 controls Ang-2 expression and modulates angiogenesis, vascular patterning, remodeling, and functions in adipose tissue. *Proc. Natl. Acad. Sci. U.S.A.* **105**, 10167–10172 (2008), 10.1073/pnas.0802486105.
33. K. Hosaka *et al.*, Tumour PDGF-BB expression levels determine dual effects of anti-PDGF drugs on vascular remodelling and metastasis. *Nat. Commun.* **4**, 2129 (2013), 10.1038/ncomms3129.
34. C. C. Leow *et al.*, MEDI3617, a human anti-angiopoietin 2 monoclonal antibody, inhibits angiogenesis and tumor growth in human tumor xenograft models. *Int. J. Oncol.* **40**, 1321–1330 (2012).
35. T. E. Peterson *et al.*, Dual inhibition of Ang-2 and VEGF receptors normalizes tumor vasculature and prolongs survival in glioblastoma by altering macrophages. *Proc. Natl. Acad. Sci. U.S.A.* **113**, 4470–4475 (2016), 10.1073/pnas.1525349113.
36. J. Folkman, Tumor angiogenesis: Therapeutic implications. *N. Engl. J. Med.* **285**, 1182–1186 (1971).
37. Y. Cao, Antiangiogenic cancer therapy: Why do mouse and human patients respond in a different way to the same drug? *Int. J. Dev. Biol.* **55**, 557–562 (2011), 10.1387/ijdb.103236yc.
38. A. Bagri *et al.*, Effects of anti-VEGF treatment duration on tumor growth, tumor regrowth, and treatment efficacy. *Clin. Cancer Res.* **16**, 3887–3900 (2010), 10.1158/1078-0432.Ccr-09-3100.
39. M. R. Junttila, F. J. de Sauvage, Influence of tumour micro-environment heterogeneity on therapeutic response. *Nature* **501**, 346–354 (2013), 10.1038/nature12626.
40. M. Shibuya, VEGF-VEGFR signals in health and disease. *Biomol. Ther. (Seoul)* **22**, 1–9 (2014).
41. Y. Liu *et al.*, Recent progress on vascular endothelial growth factor receptor inhibitors with dual targeting capabilities for tumor therapy. *J. Hematol. Oncol.* **15**, 89 (2022), 10.1186/s13045-022-01310-7.
42. D. Ribatti, T. Annese, S. Ruggieri, R. Tamma, E. Crivellato, Limitations of anti-angiogenic treatment of tumors. *Transl. Oncol.* **12**, 981–986 (2019), 10.1016/j.tranon.2019.04.022.
43. J. M. Munson *et al.*, Anti-invasive adjuvant therapy with imipramine blue enhances chemotherapeutic efficacy against glioma. *Sci. Transl. Med.* **4**, 127ra136 (2012), 10.1126/scitranslmed.3003016.
44. M. Mofarrahi, S. N. Hussain, Expression and functional roles of angiopoietin-2 in skeletal muscles. *PLoS One* **6**, e22882 (2011).
45. J. Durham-Lee, Y. Wu, V. Mokkapati, A. Paulucci-Holthauzen, O. Nesic, Induction of angiopoietin-2 after spinal cord injury. *Neuroscience* **202**, 454–464 (2012).
46. M. Schmittnaegel *et al.*, Dual angiopoietin-2 and VEGFA inhibition elicits antitumor immunity that is enhanced by PD-1 checkpoint blockade. *Sci. Transl. Med.* **9**, eaak9670 (2017).
47. K. Hosaka *et al.*, Pericyte–fibroblast transition promotes tumor growth and metastasis. *Proc. Natl. Acad. Sci. U.S.A.* **113**, E5618–E5627 (2016).
48. B. N. Perry *et al.*, Pharmacologic blockade of angiopoietin-2 is efficacious against model hemangiomas in mice. *J. Invest. Dermatol.* **126**, 2316–2322 (2006), 10.1038/sj.jid.5700413.
49. A. Stratmann, W. Risau, K. H. Plate, Cell type-specific expression of angiopoietin-1 and angiopoietin-2 suggests a role in glioblastoma angiogenesis. *Am. J. Pathol.* **153**, 1459–1466 (1998).
50. I. Helfrich *et al.*, Angiopoietin-2 levels are associated with disease progression in metastatic malignant melanoma. *Clin. Cancer Res.* **15**, 1384–1392 (2009).
51. E. Obaia, T. Mohsen, A. Abou Zeid, Tumor-derived vascular endothelial growth factor and angiopoietin-2 in non-small cell lung cancer. *Bull. Egyptian Soc. Physiol. Sci.* **27**, 277–292 (2007).
52. S. Hong *et al.*, Expressions and clinical significances of angiopoietin-1, angiopoietin-2, and Tie-2 receptor in patients with colorectal cancer. *Ann. Coloproctol.* **33**, 9 (2017).
53. J. Urosevic *et al.*, ERK1/2 signaling induces upregulation of ANGPT2 and CXCR4 to mediate liver metastasis in colon cancer. *Cancer Res.* **80**, 4668–4680 (2020), 10.1158/0008-5472.Can-19-4028.
54. A. Dowlati *et al.*, A phase I, first-in-human study of AMG 780, an angiopoietin-1 and -2 inhibitor, in patients with advanced solid tumors. *Clin. Cancer Res.* **22**, 4574–4584 (2016), 10.1158/1078-0432.Ccr-15-2145.
55. K. P. Papadopoulos *et al.*, A phase I first-in-human study of Nesvacumab (REGN910), a fully human anti-angiopoietin-2 (Ang2) monoclonal antibody, in patients with advanced solid tumors. *Clin. Cancer Res.* **22**, 1348–1355 (2016), 10.1158/1078-0432.Ccr-15-1221.
56. J. Mooi *et al.*, Dual Antiangiogenesis Agents Bevacizumab Plus Trebananib, without Chemotherapy, in First-line Treatment of Metastatic Colorectal Cancer: Results of a Phase II Study *Clin. Cancer Res.* **27**, 2159–2167 (2021), 10.1158/1078-0432.Ccr-20-2714.